J. Biochem. 92, 1049-1057 (1982)

Analyses of Optical Absorption and Circular Dichroism Spectra of Spinach Ferredoxin at Alkaline pH

Hideyo HASUMI

Department of Biophysical Chemistry, Kitasato University School of Medicine, Sagamihara, Kanagawa 228

Received for publication, March 17, 1982

The whole protein structure and the microenvironments of the iron-sulfur cluster and of the side chains of amino acid residues of spinach ferredoxin were studied by optical absorption and circular dichroism (CD) spectroscopy in the alkaline pH range.

From the pH-dependence of the optical absorption changes at 245 nm, the four tyrosyl residues of ferredoxin were classified into three groups: one exposed residue with a normal apparent *pK* value of 10.1, two exposed residues with abnormal apparent *pK* values of 12.0, and one buried residue showing time-dependent ionization. The absorption in the visible region disappeared gradually with the ionization of the buried residue rather than that of the three exposed residues. The apparent *pK* value of 10.0 was obtained from the rapid CD changes at 258 nm caused by pH elevation from neutral to alkaline pH. The structural alteration associated with the CD change had no effect on the secondary structure of the protein moiety other than the iron-sulfur cluster and the microenvironment of the cluster. The rate constants obtained from the time courses of the CD changes in the near-ultraviolet and visible regions were in good agreement with those obtained from the time courses of the optical absorption changes.

These results lead to the conclusions that (1) the native ferredoxin structure is maintained through the interaction with the iron-sulfur cluster and (2) the protein structure in the neighborhood of the cluster, important for the physiological activity, is not perturbed even though the exposed tyrosyl residues are ionized.

Spinach ferredoxin has been reported to have an iron-sulfur cluster which consists of two iron atoms, two labile sulfur atoms, and four cysteinyl residues (*1*). The amino acid sequence of the ferredoxin has been determined (*2*). By using a solvent perturbation technique with 20% ethylene glycol, Hasumi and Nakamura (*3*) have shown that (1) three of four tyrosyl residues of the ferredoxin are exposed on the surface of the protein molecule and one tyrosyl residue is buried in a region deeply folded into the protein framework, and (2) the tryptophyl residue of this protein is in a 'half-buried' state. On the basis of a model of the secondary structure of the ferredoxin predicted from its primary structure, Tyr-3, Tyr-37, and Tyr-80 have been proposed to be the exposed residues

and Tyr-23 to be the buried residue (*3*). The detailed three-dimensional structure of spinach ferredoxin has not yet been established by X-ray crystallography. However, Fukuyama and coworkers (*4*, *5*), using X-ray analyses, have recently reported the three-dimensional structure of *Spirulina platensis* ferredoxin, a chloroplast-type ferredoxin having an iron-sulfur cluster and an amino acid sequence similar to those of spinach ferredoxin (*2*, *6*). This will provide valuable clues as to the structure of spinach ferredoxin.

The optical absorption and circular dichroism (CD) in the visible region due to the iron-sulfur cluster of ferredoxin have been utilized for studying the microenvironment of the cluster (*3*, *7–14*). On the other hand, the optical absorption and CD in the near-ultraviolet region have been generally used for studying the protein structure and the states of side chains of amino acid residues (*15–27*). In particular, the ionization of phenolic hydroxyl groups of tyrosyl residues is reflected in the optical absorption changes at 245 and 295 nm (*15–20*) and the conformational changes caused by a pH-jump have been monitored by following the time-dependent optical absorption changes at 245 and 295 nm (*16*, *17*, *19*). In the present study, the whole protein structure and the microenvironments of the iron-sulfur cluster and tyrosyl residues of spinach ferredoxin were investigated by monitoring the optical absorption and CD changes in the visible and near-ultraviolet regions after a pH-jump.

MATERIALS AND METHODS

Ferredoxin was purified from spinach leaves by a method similar to that described by Tagawa and Arnon (*28*). The concentration of this protein was estimated using a molar extinction coefficient of 9.68 $mM^{-1} \cdot cm^{-1}$ at 420 nm (*29*).

The optical absorption and CD measurements were made with a Union Giken SM-401 high-sensitivity double-beam spectrophotometer and a Union Giken Dichrograph III-J, respectively, at 25°C. Both machines were coupled with a computer, Union Giken system-77. The CD stopped-flow measurements were made with the above CD spectrophotometer equipped with a Union Giken stopped-flow apparatus, RA-411. The optical absorption stopped-flow measurements were made with a Union Giken rapid scan reaction analyzer, RA-1300. The improvement of the signal-to-noise ratio of a CD stopped-flow trace was carried out by a 7-point least-squares smoothing as described by Savitzky and Golay (*30*). The molar ellipticities were calculated by use of the molecular weight of ferredoxin for the CD spectra in the near-ultraviolet and visible regions and by use of the mean residue weight of the component amino acids for the CD spectra in the far-ultraviolet region. The optical path of the observation cell was 10 mm for the optical absorption and CD measurements in the near-ultraviolet and visible regions, and 1 mm for the CD measurements in the far-ultraviolet region.

Ferredoxin was dissolved in 10 mM Tris-HCl (pH 7.4) buffer containing 0.5 M NaCl. Unless otherwise noted, 0.1 ml of the sample solution was added to 3 ml of 50 mM glycine/NaOH buffer in which the concentration of sodium ion had been adjusted to 0.45 M with NaCl. When using the stopped-flow apparatus, the sample solution was mixed one-to-one with a 0.1 M glycine/NaOH buffer in which the concentration of sodium ion had been adjusted to 0.4 M. CD measurement in the far-ultraviolet region was done by adding a small amount of 1 N NaOH to the sample solution.

The final pH of the solution was measured with a Toa Electronics pH meter, HM-5A, standardized with sodium phosphate (pH 6.86) and sodium carbonate (pH 10.02) buffers purchased from Nakarai Chemicals.

RESULTS

Optical Absorption Spectra of Ferredoxin in the Alkaline pH Range—Figure 1 shows the optical absorption spectra of ferredoxin. When the final pH was 10.38, the absorptivity around 245 nm increased but the absorptivity in the visible region was practically constant (dotted line). When the final pH was 11.10, the absorptivity around 245 nm increased further and the absorptivity in the visible region decreased (dashed and dotted line). When the final pH was 12.80, the absorption in the visible region virtually disappeared (dashed line). These results indicate that below pH 11, the iron-sulfur cluster was maintained without any significant change despite the ionization of tyrosyl residues, but above pH 11, the cluster was decom-

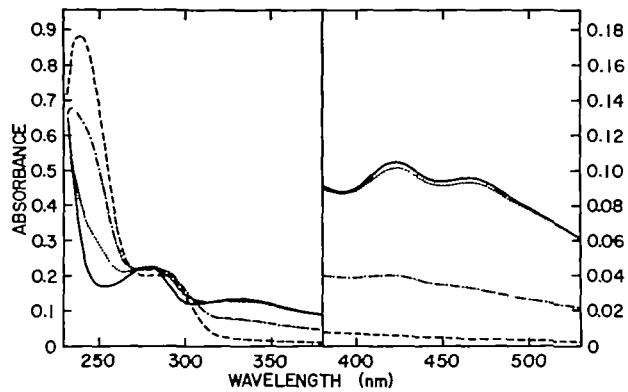

Fig. 1. Absorption spectra of ferredoxin in the alkaline pH range at 25°C. The spectra were measured at about 90 min after mixing as described in "MATERIALS AND METHODS." Ferredoxin concentration was 10.8 μM. ——, pH 7.40; ·····, pH 10.38; –·–·–, pH 11.10; – – –, pH 12.80.

posed simultaneously with further ionization of tyrosyl residues.

pH-Dependence of the Optical Absorption Changes at 245 nm—Hiromi *et al.* (*19*) reported that (1) the ionization of the originally exposed tyrosyl residues proceeded completely within the dead-time of a stopped-flow apparatus (about 2 ms), and (2) the observed time-dependent absorption change, if any, undoubtedly reflected the process of conformational change (the exposure of buried tyrosyl residues) followed by instantaneous ionization of the tyrosyl residues. In the present study, therefore, the stopped-flow apparatus was used in order to estimate the apparent pK, pK_{app}, values of the three exposed tyrosyl residues of ferredoxin. Within 0.1 s after mixing, the optical absorption in the visible region ceased to change and the absorption at 245 nm did not show time-dependent change (see below). These results suggest that the optical absorption changes at 245 nm observed within 0.1 s were predominantly due to ionization of the exposed tyrosyl residues but not appreciably due to ionization of the buried tyrosyl residue and cysteinyl residues, as reported by Donovan (*16*) (see "DISCUSSION").

Figure 2 shows the changes in the absorptivity at 245 nm as a function of pH. The data within 0.1 s after mixing (open circles) clearly showed a shoulder around pH 11, indicating that there were at least two different ionization stages. Since the absorption change around pH 11 was about one-third of that around pH 13, one stage presumably involved one residue and the other, two residues. Therefore, two pK_{app} values and a difference molar extinction coefficient at 245 nm for ionization of one tyrosyl residue, $\Delta\varepsilon_{245}^{max}$, were determined so as to give the smallest mean square error between the observed and theoretical difference absorptivities. The best fit was obtained when the two pK_{app} values were 10.1 ± 0.1 for one residue and 12.0 ± 0.1 for two residues, and $\Delta\varepsilon_{245}^{max}$ was 14.2 $mM^{-1} \cdot cm^{-1}$. The pK_{app} values of about 10 for normal exposed residues and of more than 11 for abnormal ones were reported earlier by other workers (*15*, *18*, *20*). These results indicate that the one exposed residue shows normal ionization and the two exposed residues show abnormal ionization. The $\Delta\varepsilon_{245}^{max}$ obtained in the present study was close to that reported for hen egg-white lysozyme, 13.2 $mM^{-1} \cdot cm^{-1}$ (*18*), rather than to those reported for *N*-acetyl-L-tyrosine ethyl ester, 10.66 $mM^{-1} \cdot cm^{-1}$ (*20*), for duck egg-white lysozyme, 10.8 $mM^{-1} \cdot cm^{-1}$ (*18*), and for human hemoglobin, 12.1 $mM^{-1} \cdot cm^{-1}$ (*15*).

The absorption changes at about 10 min after mixing (closed circles) are also plotted in Fig. 2. Based on $\Delta\varepsilon_{245}^{max}$ of 14.2 $mM^{-1} \cdot cm^{-1}$, the number of ionized tyrosyl residues of ferredoxin was calculated to be 4.0 at the final level, above pH 12. Accordingly, this $\Delta\varepsilon_{245}^{max}$ was used for calculation of the number of ionized tyrosyl residues throughout the present study.

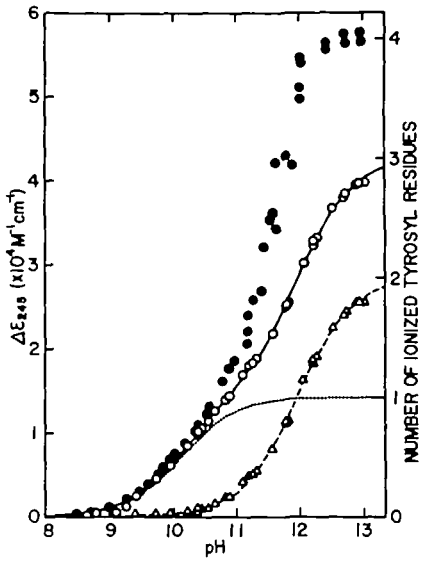

Fig. 2. Spectrophotometric titration curves of ferredoxin. The absorptivities at 245 nm within 0.1 s (○) were measured after mixing by use of the stopped-flow apparatus as described in "MATERIALS AND METHODS." The absorptivities at 10 min (●) were measured after mixing in the same manner as in Fig. 1. The absorptivity at pH 7.40 was used as a reference. Ferredoxin concentration was 9.25 μM. The solid line is the sum of the two theoretical curves drawn by using a $\Delta\varepsilon_{245}^{max}$ of 14.2 mM^{-1}·cm^{-1}, and a pK_{app} value of 10.1 for one tyrosyl residue (dotted line) and an identical pK_{app} value of 12.0 for two tyrosyl residues (dashed line). The $\Delta\varepsilon_{245}^{max}$ and two pK_{app} values were determined as described in the text. △, the calculated values obtained by subtracting the theoretical values of the dotted line from the observed values (○).

Time-Dependent Optical Absorption Changes after the pH-Jump (up) from Neutral to Alkaline pH—Figure 3 shows the time courses of the optical absorption changes at 245 (A) and 420 (B) nm after the pH-jump (up) from neutral to alkaline pH. When the final pH was 10.35, although about 0.7 residues were immediately ionized within 0.1 s after mixing, no time-dependent ionization of tyrosyl residues was subsequently detected (Fig. 3A, curve a). No significant absorption change at 420 nm was observed (Fig. 3B, curve a). When the final pH was 11.60, the rapid ionization of about 1.7 residues was followed by the very slow ionization of about 1.9 residues (Fig. 3A, curve b). The absorptivity at 420 nm decreased simultaneously with the slow ionization of tyrosyl residues (Fig. 3B, curve b). When the final pH was 12.66, the rapid ionization of about 2.7 residues was followed by the time-dependent ionization of about 1.2 residues (Fig. 3A, curve c). The absorption at 420 nm virtually disappeared in about 4 min after mixing (Fig. 3B, curve c). These results imply that the decomposition of the iron-sulfur cluster occurred simultaneously with the ionization of the buried tyrosyl residue rather than that of the exposed tyrosyl residues.

The numbers of the ionized tyrosyl residues were plotted against pH (Fig. 4). In the pH range of 11–13, the numbers of the tyrosyl residues showing the time-dependent ionization were more than one, the number of the buried tyrosyl residue. This indicates that tyrosyl residues which were

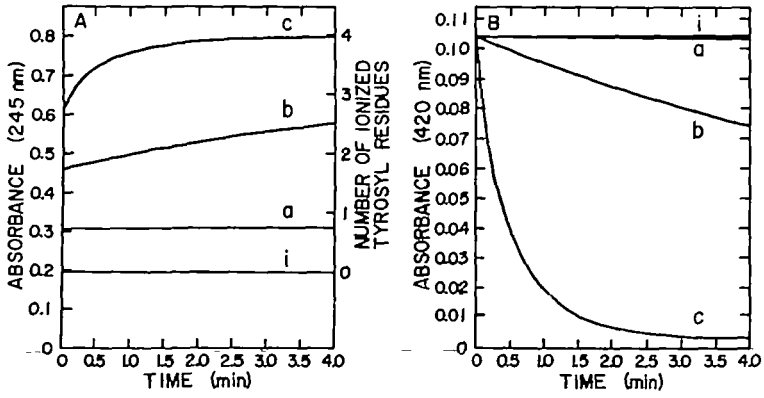

Fig. 3. Time courses of the optical absorption changes at 245 (A) and 420 (B) nm after the pH-jump (up) from neutral to alkaline pH. Measurements were made at the final pH of 10.35 (a), 11.60 (b), and 12.66 (c). Other conditions were the same as in Fig. 1. Trace i shows the initial level of the absorptivity at pH 7.40.

originally exposed but not ionizable at the pH became ionizable after the conformational change.

As shown in Fig. 5 and Table I, the apparent first-order rate constants obtained from the absorption changes at 245 nm were dependent on pH. However, the rate constants increased nonlinearly with increase in pH. It is conceivable that a certain number of ionizable groups with higher pK_{app} values (probably ammonium and/or guanidinium groups) participate cooperatively in the conformational change as described by Hiromi *et al.* (*19*). The two rate constants obtained at 245 nm and 420 nm were in good agreement, as listed in Table I. This supports the idea that the iron-sulfur cluster was decomposed simultaneously with the ionization of the tyrosyl residues which became ionizable after the conformational change of a protein moiety other than the cluster (referred to as the protein moiety in this paper).

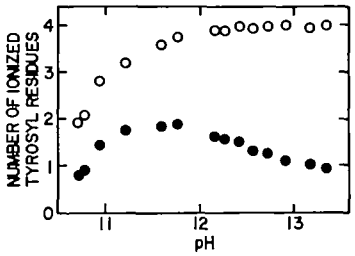

Fig. 4. pH dependence of the number of ionized tyrosyl residues. Ferredoxin concentration was 10.5 μM. Other conditions were the same as in Fig. 3. ○, the total number of the ionized tyrosyl residues, calculated from the difference between the initial level (at pH 7.40) and the final level (in 10–120 min at each pH) of the absorptivities; ●, the number of tyrosyl residues showing the time-dependent ionization, calculated from the reaction trace.

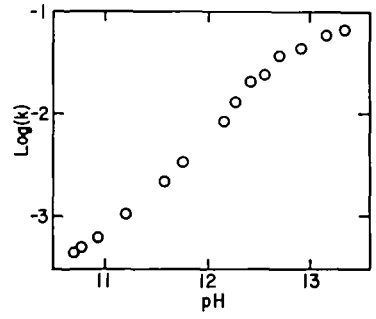

Fig. 5. pH dependence of the apparent first-order rate constants at 245 nm. Conditions were the same as in Fig. 4.

CD Spectra of Ferredoxin in the Alkaline pH Range—Figure 6 shows the CD spectra of ferredoxin in the visible and near-ultraviolet regions. When the final pH was 10.38, although the CD

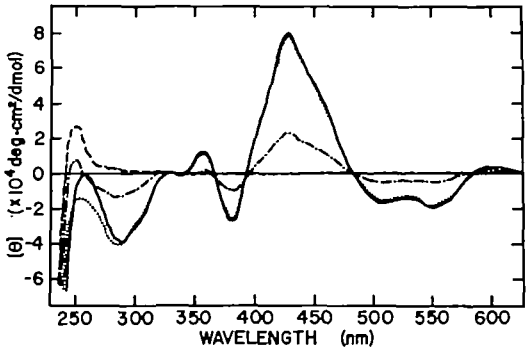

Fig. 6. CD spectra of ferredoxin in the alkaline pH range. The spectra are the averages of 2 runs in each case. Other conditions were the same as in Fig. 1. ——, pH 7.40; ·····, pH 10.38; –·–·–, pH 11.10; – – –, pH 12.80.

TABLE I. Apparent first-order rate constants for alkaline denaturation of ferredoxin. Conditions were the same as in Fig. 4. Values expressed are of $k_{obsd.}$ and are in s^{-1}.

Final pH	Optical absorption		Circular dichroism		
	245 nm	420 nm	258 nm	290 nm	428 nm
10.95	5.64×10^{-4}	5.40×10^{-4}	5.31×10^{-4}	5.13×10^{-4}	5.33×10^{-4}
11.60	2.18×10^{-3}	1.89×10^{-3}	1.84×10^{-3}	1.70×10^{-3}	1.79×10^{-3}
12.17	8.24×10^{-3}	8.13×10^{-3}	8.37×10^{-3}	8.16×10^{-3}	8.15×10^{-3}
12.56	2.39×10^{-2}	2.44×10^{-2}	2.42×10^{-2}	2.45×10^{-2}	2.43×10^{-2}
13.16	5.31×10^{-2}	5.42×10^{-2}	5.64×10^{-2}	5.55×10^{-2}	5.40×10^{-2}

bands in the visible region remained unchanged, the magnitude of negative ellipticity around 258 nm increased (dotted line). When the final pH was 11.10, the magnitudes of CD bands in the visible and near-ultraviolet regions decreased (dashed and dotted line). When the final pH was 12.80, the CD bands practically disappeared in the longer wavelength region above 270 nm (dashed line). Figure 7 shows the CD spectra of ferredoxin in the far-ultraviolet region. The CD spectrum at pH 10.16 (dotted line) was almost identical with that at pH 7.30 (solid line). In contrast, both CD spectra at pH 11.26 and 12.70 (dashed and dotted line and dashed line) showed a significant decrease in the magnitude of the negative ellipticity around 220 nm. These results indicate that (1) below pH 11, the secondary structure of the protein moiety and the microenvironment of the iron-sulfur cluster remained practically unchanged, although there was a subtle structural alteration reflected in the CD change around 258 nm, but (2) above pH 11, the secondary structure of the protein moiety and the microenvironment of the cluster changed significantly.

Time-Dependent CD Changes after the pH-Jump (up) from Neutral to Alkaline pH—Figure 8 shows the CD changes at 428 (A), 290 (B), and 258 (C) nm after the pH-jump (up) from pH 7.40 to pH 12.70. Figures 8A and 8B show that the magnitudes of the CD changes calculated from the stopped-flow traces were almost equal to the total magnitudes of the respective CD changes. However, the ellipticity at 258 nm decreased rapidly

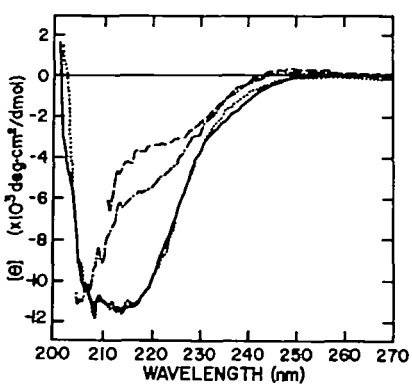

Fig. 7. CD spectra of ferredoxin in the far-ultraviolet region in the alkaline pH range at 25°C. The spectra were measured at about 90 min after mixing as described in "MATERIALS AND METHODS." The spectra are the averages of 16 runs in each case and are corrected for concentration. Ferredoxin concentration was 14.4 μM. ——, pH 7.30; ·····, pH 10.16; –·–·–, pH 11.26; – – –, pH 12.70.

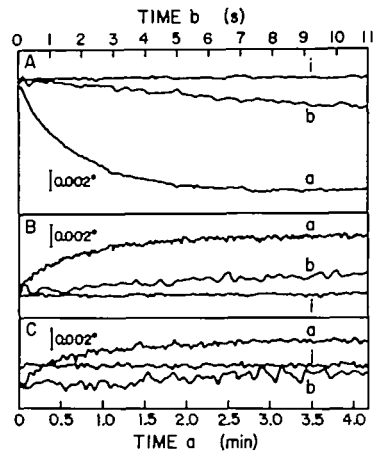

Fig. 8. Time courses of the CD changes at 428 (A), 290 (B), and 258 (C) nm after the pH-jump (up) from pH 7.40 to 12.70. Measurements were made by use of the stopped-flow apparatus as described in "MATERIALS AND METHODS." Ferredoxin concentration was 15.6 μM. The traces are of a single run (a) and the averages of 4 runs (b) in each case. Trace i shows the initial level of the ellipticity at pH 7.40.

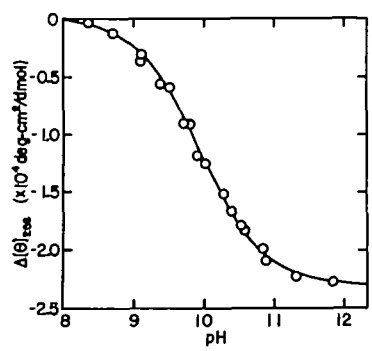

Fig. 9. Difference ellipticities at 258 nm as a function of pH. The ellipticities are the averages of those within 5 s after mixing. The ellipticity at pH 7.40 was used as a reference. Ferredoxin concentration was 11.0 μM. Other conditions were the same as in Fig. 8. The solid line is a theoretical curve drawn by using a pK_{app} value of 10.0 and a maximum difference ellipticity of −23,100 deg·cm²/dmol. The pK_{app} value and the maximum difference ellipticity were determined so as to give the smallest mean square error between the observed and theoretical difference ellipticities.

within the dead-time of the apparatus (about 2 ms) and then increased (Fig. 8C). This suggests that even above pH 12, there was the subtle structural alteration as observed below pH 11. As listed in Table I, the rate constants obtained from the CD traces at 428, 290, and 258 nm were in good agreement with one another, and also with those obtained from the optical absorption experiments. These results indicate that the conformational changes of ferredoxin can be monitored by using the time-dependent absorption change as a probe, as reported by other workers (*16*, *17*, *19*).

pH-Dependence of the Difference Ellipticity at 258 nm—The CD changes at 258 nm within 5 s after mixing by means of the stopped-flow apparatus were plotted against pH (Fig. 9). The pK_{app} value of 10.0 ± 0.1 was obtained from the figure. This pK_{app} value is in good agreement with that of 10.1 obtained from the optical absorption experiment. This suggests that the structural alteration reflected in the CD change is associated with the ionization of the normal exposed tyrosyl residue.

DISCUSSION

By the stopped-flow method, the pK_{app} values of the three exposed tyrosyl residues of spinach ferredoxin were estimated to be 10.1 for one tyrosyl residue and 12.0 for two tyrosyl residues (Fig. 2). These pK_{app} values are considered to be those of tyrosyl residues in the native protein molecule as judged from the findings that the whole protein structure and the microenvironment of the iron-sulfur cluster remained practically unchanged within the time scale used for estimation of the pK_{app} values (Figs. 3 and 8). Inouye *et al.* (*20*) reported that the observed difference in pK_{app} values resulted from differences in microscopic electrostatic field or the presence of hydrogen bonds. It is thus conceivable that one exposed tyrosyl residue is normally ionized but two exposed tyrosyl residues are abnormally ionized because of the interaction with other parts of the protein. From X-ray analyses of *Spirulina platensis* ferredoxin and molecular evolutional studies on chloroplast-type ferredoxins, Fukuyama *et al.* (*4*) concluded that most of the invariant residues were around the iron-sulfur cluster and the segments from Pro-38 to Cys-49 and from Thr-78 to Ala-81 must be important in stabilizing the cluster cavity. These considerations imply that both Tyr-39 and Tyr-82, which correspond to Tyr-37 and Tyr-80, respectively, in spinach ferredoxin (*2*, *6*), are located close to the cluster and may interact with other parts of the protein. In contrast, Tyr-3, which is at the corresponding position in spinach ferredoxin, is located adjacent to the positively charged Lys-4 and very close to the N-terminal region (*2*, *6*). It is therefore possible that Tyr-3 is the exposed tyrosyl residue with a normal pK_{app} value of 10.1, and Tyr-37 and Tyr-80 are the exposed tyrosyl residues with abnormal pK_{app} values of 12.0.

Donovan (*16*) reported that $\Delta\varepsilon_{243}^{max}$ for ionization of one cysteinyl residue of aldolase was 3.80 $mM^{-1} \cdot cm^{-1}$ in water. In the case of spinach ferredoxin, the ionization of cysteinyl residues is considered to make practically no contribution to the optical absorption change at 245 nm for the following two reasons. (1) Within the time scale (0.1 s after mixing) used for calculation of $\Delta\varepsilon_{245}^{max}$, no significant absorption changes at 420 nm were observed (Fig. 3), indicating that four cysteinyl residues participating in the iron-sulfur cluster were not ionized. On the other hand, the one remaining cysteinyl residue was proposed to be buried because of its low reactivity toward *p*-chloromercuribenzoate in the native molecule (*3*). Therefore, the residue should remain neutral within 0.1 s and show time-dependent ionization, if any. (2) The iron-sulfur cluster and the protein structure were completely decomposed at the final level, above pH 12 (Figs. 3 and 8). The absorption change at the final level should be greater than the observed change if the ionization of the cysteinyl residues contributed to the absorption change. On the basis of $\Delta\varepsilon_{245}^{max}$ of 14.2 $mM^{-1} \cdot cm^{-1}$, however, the number of ionized tyrosyl residues at the final level was found to be 4.0, the total number of tyrosyl residues of ferredoxin.

It is well known that the near-ultraviolet CD band ascribable to tyrosyl residue exhibits a red shift with increase in pH (*22*, *23*). However, the near-ultraviolet CD band of ferredoxin showed a blue shift rather than a red shift (Fig. 6, dotted line) and rapid CD changes around 258 nm were observed after the pH-jump (up) from neutral to alkaline pH (Fig. 6, dotted line and Fig. 8C).

These results were similar to those for insulin (*24*, *25*). The near-ultraviolet CD band of insulin is reported to be due to the disulfide bond (*24*), and due to tyrosyl and phenylalanyl residues (*25*). Spinach ferredoxin has no disulfide bond (*2*). In the present study, the pK_{app} value of 10.0 obtained from the CD changes at 258 nm was in good agreement with that of 10.1 for the normal exposed tyrosyl residue (Figs. 2 and 9). These results suggest that the negatively charged tyrosyl residue, which exhibits no ellipticity around 258 nm in the non-ionized state, interacts electrostatically with a positively charged residue in the neighborhood and acquires optical activity. Tyr-3 and Lys-4 are the most likely candidates for the electrostatically interacting residues, since (1) the ionization of the tyrosyl residue had no effect on the secondary structure of the protein moiety and the microenvironment of the iron-sulfur cluster (Figs. 6, 7, and 8), and (2) Tyr-3 and Lys-4 are adjacent residues in the N-terminal regions of spinach and *Spirulina platensis* ferredoxins (*2*, *6*) and protrude into the solvent region under the lower part (far apart from the cluster) of a β-barrel-like structure (*5*). These lines of consideration support the view that Tyr-3 is the exposed tyrosyl residue with a normal pK_{app} value of 10.1.

Tryptophyl residues have optical activity around 290 nm (*21*, *23*, *26*, *27*). Adrenodoxin, which has an iron-sulfur cluster similar to that of ferredoxin (*8*, *14*) and has a single tyrosyl residue but no tryptophyl residue (*31*), is reported to exhibit no CD band around 290 nm like that of ferredoxin (*8*, *32*). These results indicate that the negative CD band around 290 nm of spinach ferredoxin is predominantly associated with the 'half-buried' tryptophyl residue rather than the iron-sulfur cluster and the tyrosyl residue. The CD band disappeared only upon unfolding of the polypeptide chain (Figs. 6, 7, and 8, and Table I). It is therefore conceivable that the CD band is sensitive to structural change of the polypeptide chain.

In the previous study (*13*), it was concluded that the native ferredoxin structure is maintained through the interaction with the iron-sulfur cluster. This remains valid, since (1) the subtle structural alteration in the N-terminal region gave rise to no significant changes in the whole protein structure and the microenvironment of the cluster, and (2) the structural changes of the protein moiety resulting in the exposure of the buried tyrosyl residue decomposed the cluster. In addition, these results lead to the conclusion that the protein structure in the neighborhood of the cluster, which is important for the physiological activity of ferredoxin, is not perturbed even though the exposed tyrosyl residues are ionized.

The author is deeply indebted to Professor S. Nakamura and Dr. H. Suzuki for their valuable advice and discussions throughout the course of this work. The author also wishes to thank Professor H. Hatano, the University of Kyoto, for his interest and encouragement during this work.

REFERENCES

1. Johnson, C.E., Cammack, R., Rao, K.K., & Hall, D.O. (1971) *Biochem. Biophys. Res. Commun.* **43**, 564–574
2. Matsubara, H. & Sasaki, R.M. (1968) *J. Biol. Chem.* **243**, 1732–1757
3. Hasumi, H. & Nakamura, S. (1978) *J. Biochem.* **84**, 707–717
4. Fukuyama, K., Hase, T., Matsumoto, S., Tsukihara, T., Katsube, Y., Tanaka, N., Kakudo, M., Wada, K., & Matsubara, H. (1980) *Nature* **286**, 522–524
5. Tsukihara, T., Fukuyama, K., Nakamura, M., Katsube, Y., Tanaka, N., Kakudo, M., Wada, K., Hase, T., & Matsubara, H. (1981) *J. Biochem.* **90**, 1763–1773
6. Wada, K., Hase, T., Tokunaga, H., & Matsubara, H. (1975) *FEBS Lett.* **55**, 102–104
7. Garbett, K., Gillard, R.D., Knowles, P.F., & Stangroom, J.E. (1967) *Nature* **215**, 824–828
8. Kimura, T. (1968) *Structure and Bonding* **5**, 1–40
9. Petering, D. & Palmer, G. (1970) *Arch. Biochem. Biophys.* **141**, 456–464
10. Petering, D., Fee, J.A., & Palmer, G. (1971) *J. Biol. Chem.* **246**, 643–653
11. Matsubara, H., Wada, K., & Masaki, R. (1976) *Adv. Exp. Med. Biol.* **74**, 1–15
12. Masaki, R., Wada, K., & Matsubara, H. (1977) *J. Biochem.* **81**, 1–9
13. Hasumi, H., Nakamura, S., Koga, K., & Yoshizumi, H. (1979) *Biochem. Biophys. Res. Commun.* **87**, 1095–1101
14. Hasumi, H., Nakamura, S., Koga, K., Yoshizumi, H., Parcells, J.H., & Kimura, T. (1982) *J. Biochem.* **91**, 135–141
15. Hermans, J., Jr. (1962) *Biochemistry* **1**, 193–196
16. Donovan, J.W. (1964) *Biochemistry* **3**, 67–74
17. Tachibana, A. & Murachi, T. (1966) *Biochemistry* **5**, 2756–2763

18. Tojo, T., Hamaguchi, K., Imanishi, M., & Amano, T. (1966) *J. Biochem.* **60**, 538–542
19. Hiromi, K., Ohnishi, M., Kanaya, K., & Matsumoto, T. (1975) *J. Biochem.* **77**, 957–963
20. Inouye, K., Tonomura, B., Hiromi, K., Sato, S., & Murao, S. (1977) *J. Biochem.* **82**, 1207–1215
21. Townend, R., Kumosinski, T.F., & Timasheff, S.N. (1967) *J. Biol. Chem.* **242**, 4538–4545
22. Simmons, N.S. & Glazer, A.N. (1967) *J. Am. Chem. Soc.* **89**, 5040–5042
23. Ikeda, K. & Hamaguchi, K. (1969) *J. Biochem.* **66**, 513–520
24. Beychok, S. (1965) *Proc. Natl. Acad. Sci. U.S.* **53**, 999–1006
25. Morris, J.W.S., Mercola, D.A., & Arquilla, E.R. (1968) *Biochim. Biophys. Acta* **160**, 145–150
26. Myer, Y.P. (1968) *Biochemistry* **7**, 765–776
27. Hasumi, H. (1980) *Biochim. Biophys. Acta* **626**, 265–276
28. Tagawa, K. & Arnon, D.I. (1962) *Nature* **195**, 537–543
29. Tagawa, K. & Arnon, D.I. (1968) *Biochim. Biophys. Acta* **153**, 602–613
30. Savitzky, A. & Golay, M.J.E. (1964) *Anal. Chem.* **36**, 1627–1639
31. Tanaka, M., Haniu, M., Yasunobu, K.T., & Kimura, T. (1973) *J. Biol. Chem.* **248**, 1141–1157
32. Sakamoto, H., Ichikawa, Y., Yamano, T., & Takagi, T. (1981) *J. Biochem.* **90**, 1445–1452